PHYSICAL REVIEW A, VOLUME 65, 011801(R)

Bistability and instability of three-level atoms inside an optical cavity

Hai Wang,* D. J. Goorskey, and Min Xiao†
Department of Physics, University of Arkansas, Fayetteville, Arkansas 72701
(Received 16 July 2001; published 11 December 2001)

Optical bistability and dynamic instability are experimentally observed and studied in a system consisting of three-level Λ-type rubidium atoms in an optical ring cavity. The bistable behavior and self-pulsing frequency are experimentally manipulated by changing the controlling and cavity field parameters (power and frequency). These nonlinear effects are influenced by the enhanced Kerr nonlinearity due to atomic coherence in such a system.

DOI: 10.1103/PhysRevA.65.011801 PACS number(s): 42.65.Pc, 42.65.Sf, 42.50.Gy

When two-level atoms couple with an optical cavity, many interesting effects occur. For example, bistable states appear in the cavity output intensity for a certain range of input intensities [1] and the output field can become unstable in the upper branch of the bistable curve under certain conditions [2]. Bistability and instability were also observed in cold clouds of cesium atoms inside an optical cavity, where degenerate Zeeman sublevels participate in the dynamic processes [3]. In that experiment, one circularly polarized laser beam was injected into the optical cavity, which interacts with all the Zeeman sublevels of the $6S_{1/2}$ $F=4$ and $6P_{3/2}$ $F=5$ states in cesium atoms. The dynamic instability was attributed to the competition between optical pumping to state $6S_{1/2}$ $F=4$, $m_F=4$ from all other Zeeman sublevels and nonlinearities due to saturation of the optical transition (from $6S_{1/2}$ $F=4$, $m_F=4$ to $6P_{2/3}$ $F=5$, $m_F=5$). However, since both optical pumping and saturation inside the optical cavity were generated by the same input laser beam, the two competing dynamic processes could not be separately controlled. Also, the trapping beams and the repumping beam in that experiment for creating the cold atomic clouds bring more complications and limitations to the understanding of these bistable and dynamic instability behaviors.

In recent years, electromagnetically induced transparency and related effects in three-level atomic systems have been studied extensively [4–6]. Many experimental demonstrations of enhancing nonlinear optical processes (such as four-wave mixing, harmonic generations, and two-photon absorption) were reported in the literature [7–11]. Recently, we have studied cavity linewidth narrowing due to the sharp dispersion change in three-level Λ-type rubidium atoms inside an optical ring cavity [12] and directly measured the Kerr-nonlinear coefficient near resonance [13]. In this paper, we report our recent experimental observations of optical bistability and dynamic instability with three-level rubidium atoms inside an optical ring cavity. Due to the exact knowledge of the Kerr-nonlinear coefficient at different controlling (or coupling) and cavity (or probe) field parameters, such as optical powers and frequency detunings [13], we can control and manipulate the bistable and unstable behaviors in such a system by simply tuning these experimental parameters.

Our basic experimental setup is shown in Fig. 1. The optical ring cavity is about 37 cm long and is composed of three mirrors. The flat mirror $M1$ and the concave mirror $M2$ ($R=10$ cm) have about a 1 and 3 % transmissivity, respectively, while the third mirror is concave ($R=10$ cm) with a reflectivity larger than 99.5% and is mounted on a piezoelectric transducer (PZT). The empty cavity finesse was measured to be about 100 with a free spectral range of 822 MHz. The rubidium vapor cell is 5 cm long with Brewster windows and is wrapped in μ metal for magnetic shielding and heat tape for atomic density control. The experiment was conducted at a vapor cell temperature of about 70 °C. One laser beam enters the cavity through mirror $M2$ and circulates inside the cavity. Another beam, i.e., the controlling field, is introduced through the polarizing beam splitter (PBS) with an orthogonal polarization to the first (cavity field) beam. The controlling beam is misaligned from the cavity field beam by a 2° angle and does not circulate inside the ring cavity. The radii of the controlling and cavity field beams at the center of the Rb vapor cell are estimated to be 700 and 80 μm, respectively. With insertion losses of the PBS and reflection losses from the vapor cell windows, we find the cavity finesse to be degraded to about 50 at a frequency far from atomic resonance.

Both lasers are extended cavity diode lasers. The controlling field is tuned to the $5S_{1/2}$ $F=2\leftrightarrow 5P_{1/2}$ $F=2$ transition, while the cavity field is tuned to the $5S_{1/2}$ $F=1\leftrightarrow 5P_{1/2}$ $F=2$ transition in ^{87}Rb, as in Ref. [12]. Both lasers are frequency locked to Fabry-Perot cavities. Their frequency de-

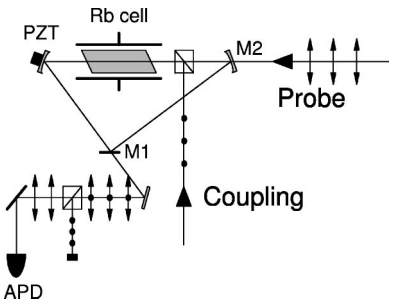

FIG. 1. Experimental setup. $M1$ and $M2$ are mirrors; PZT is a mirror mounted on a piezoelectric transducer; APD is an avalanche photodiode detector.

*Permanent address: Institute of Optoelectronics, Shanxi University, Taiyuan 030006, China.
†Email address: mxiao@uark.edu

tunings from their respective atomic transitions are set using saturation absorption spectroscopy. One of the key advantages of the current system is the use of the two-photon Doppler-free configuration [6]. By propagating the controlling and cavity fields colinearly through the vapor cell containing three-level Λ-type rubidium atoms, we do not need to use atomic beams or cooled atomic samples to eliminate the first-order Doppler effect.

With both lasers frequency locked, the length of the cavity is scanned across its resonance by applying a ramp voltage to the PZT on one of the cavity mirrors. The cavity transmission is measured by an avalanche photodiode (APD). Without the controlling field, the cavity transmission profile is basically symmetric. When the controlling field is present, the cavity transmission profile becomes asymmetric due to the enhanced Kerr nonlinearity in which the index of refraction of the atomic vapor is dependent on the intensity of the cavity field (I_p) according to $n=n_0+n_2I_p$. The degree of asymmetry in the cavity transmission profile is a direct measure of the nonlinear phase shift and is proportional to the Kerr-nonlinear index of refraction n_2 [13]. As the cavity length is scanned from longer to shorter, the cavity will take a longer time to reach the peak power on resonance if n_2 is positive, which can be seen in the simple expression for cavity phase detuning $\delta=-2\pi(t-t_0)/\tau+2\pi\ell n_2 I_p/\lambda$, where τ is the time period between two transmission peaks when the cavity length is scanned, ℓ is the length of the Rb cell, and $t-t_0$ in the first term is the time scanning through the cavity length with t_0 as a reference time. When the intracavity intensity increases (as the phase detuning approaches zero), the nonlinear phase shift in the second term (proportional to the increased intensity I_p) will act against the increase since the second term has an opposite sign ($n_2>0$) to the first one causing the cavity to take a longer time to reach resonance. When the cavity is scanned passing its resonance, the cavity field intensity will decrease, which will speed up the time for the cavity to become off resonant (i.e., the intenstiy drops off sharply). When n_2 is negative and the cavity is scanned from shorter to longer (the first term has a positive sign in this case), the asymmetry in the cavity transmission will behave in a similar fashion. However, if the two terms have the same signs, the cavity transmission will rise sharply, but fall off slowly. In a previous paper [13], we measured n_2 as a function of probe and coupling detunings (Δ_p and Δ_c), respectively. In general, the Kerr-nonlinear coefficient n_2 is dependent on the detunings as well as the intensity of the controlling field. Adjusting these parameters offers sufficient control over bistable and unstable behaviors.

As the cavity length is scanned from longer to shorter (with a scan rate of 0.45 μm/ms and $n_2>0$), the cavity transmission profile becomes asymmetric, reaching its maximum value much later than if $n_2=0$. The upper trace of Fig. 2 shows this clearly for a controlling field detuning of $\Delta_c=+7$ MHz and a cavity field detuning of $\Delta_p=0$, which correspond to maximum positive Kerr nonlinearity under such conditions. In this trace, the injected controlling power into the atomic cell was about 18.5 mW corresponding to an average Rabi frequency of $\Omega_c=2\pi\times 69$ MHz at the center of the Rb vapor cell. The peak intracavity power (with cavity

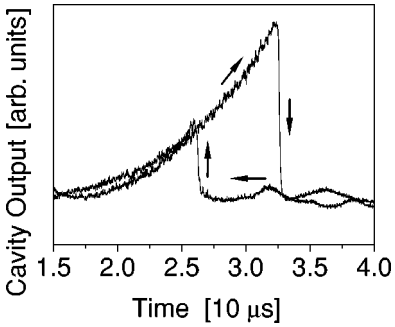

FIG. 2. Cavity transmission profile showing bistability for $P_p^{IN}=0.30$ mW, $P_c=18.5$ mW, $\Delta_p=0$, and $\Delta_c=+7$ MHz. Upper trace is when cavity length is scanned from shorter to longer. Lower trace is the opposite. ($n_2>0$ in both cases.)

on resonance) was estimated to be about 20 μW for the upper trace, which corresponds to a Rabi frequency of $\Omega_p=2\pi\times 20$ MHz at the center of the Rb vapor cell. For the same conditions, when the cavity is scanned from shorter to longer (still $n_2>0$), the cavity transmission intensity takes the lower trace in Fig. 2, which rises sharply and falls off gradually at a much later time. This hysteresis is a clear indication of optical bistability for the intracavity field. The bistability range and thresholds may be manipulated by the controlling and cavity field intensities and their frequency detunings. We searched the parameter spaces and found that the bistable region (positions between the lower and upper turning points) was maximum under the above experimental conditions. Furthermore, the bistability occurs at a quite low-intracavity intensity due to the enhanced Kerr nonlinearity near resonance. By changing the sign of n_2 (setting the controlling and/or cavity field frequency detunings to different values) [13], we may dramatically change the shape of the bistability curve.

Oscillation, or self pulsing, occurs in the cavity transmission intensity when the intensity of the controlling field is increased above a certain threshold value. This threshold value is determined by the cavity input power P_p^{IN} and frequency detunings of the controlling and cavity fields, Δ_p and Δ_c. When the controlling intensity is increased further beyond a certain value, the oscillations disappear. In Fig. 3, the cavity transmissions for increased controlling power are shown for $\Delta_p=+20$ MHz and $\Delta_c=0$. The cavity input power was $P_p^{IN}=0.55$ mW before entering the cavity. The oscillation time period and amplitude increase with increasing controlling power, while the duration of self pulsing is longer for low-controlling powers and becomes shorter as the controlling power increases, until the oscillations finally stop when the controlling power reaches $P_c=17.1$ mW.

For a fixed controlling intensity and a given set of controlling and cavity field frequency detunings Δ_p and Δ_c, the cavity transmission shows an opposite behavior as the cavity input intensity increases. As the cavity input intensity is increased, passing a threshold value, oscillations begin to occur. The time period of the oscillations decreases as the cavity input power increases until finally the oscillations stop at a higher cavity input power of $P_p^{IN}=1.86$ mW. The oscillation amplitude also decreases, relative to the cavity transmis-

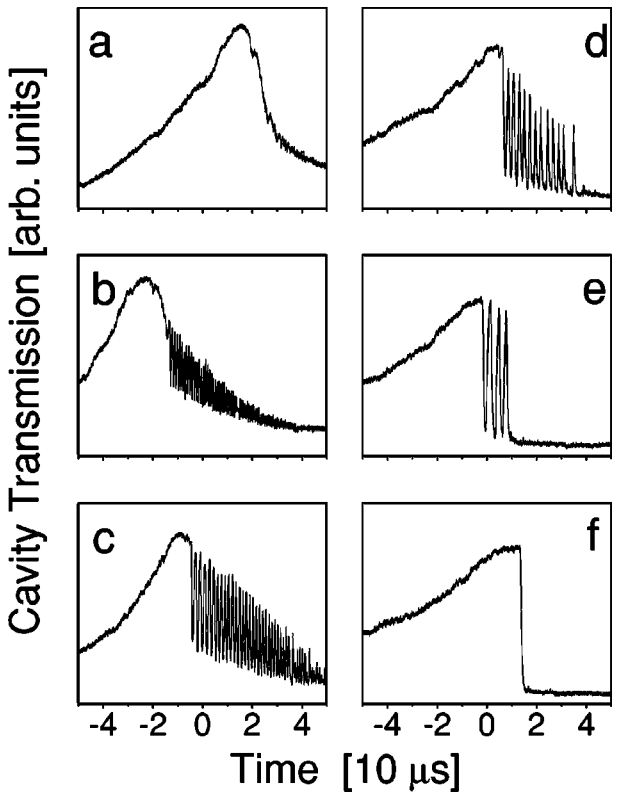

FIG. 3. Cavity transmission profiles for $P_p^{IN}=0.55$ mW, $\Delta_p=+20$ MHz, $\Delta_c=0$, and (a) $P_c=1.48$ mW; (b) $P_c=2.21$ mW; (c) $P_c=5.47$ mW; (d) $P_c=12.2$ mW; (e) $P_c=15.4$ mW; (f) $P_c=17.1$ mW.

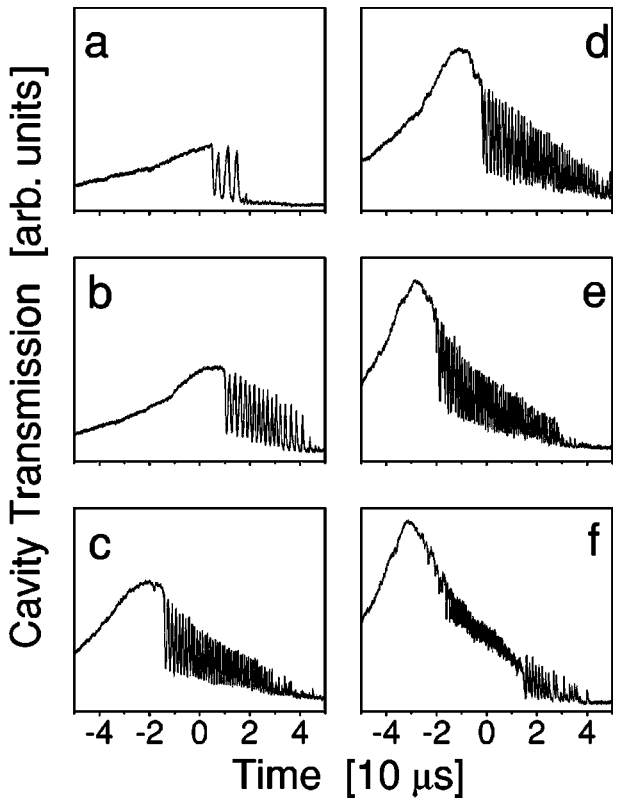

FIG. 4. Cavity transmission profiles for $P_c=8.7$ mW, $\Delta_p=+20$ MHz, $\Delta_c=0$, and (a) $P_p^{IN}=0.37$ mW; (b) $P_p^{IN}=0.56$ mW; (c) $P_p^{IN}=0.91$ mW; (d) $P_p^{IN}=1.22$ mW; (e) $P_p^{IN}=1.55$ mW; (f) $P_p^{IN}=1.86$ mW.

sion peak, as the input cavity intensity increases. This behavior can be seen from Fig. 4 in which cavity transmission profiles are shown for the same controlling and cavity field detunings as in Fig. 3, but for a controlling power fixed at $P_c=8.7$ mW. In Figs. 4(a)–4(f), the cavity input power is increased from $P_p^{IN}=0.37$ mW to $P_p^{IN}=1.86$ mW. Since it is the cavity field's output from the ring cavity that is being measured, the on-resonance transmission peaks in Fig. 4 are increasing with increasing cavity input power. It is interesting to point out that the lower threshold in Fig. 4(a) is similar to the upper threshold in Fig. 3(e), while the upper threshold in Fig. 4(f) is comparable to the lower threshold in Fig. 3(b), in the sense that the shapes of the cavity transmission profiles are similar. We have also mapped out the oscillation regions for other parameters, i.e., frequency detunings Δ_p and Δ_c. With these experimental parameters, we can easily control the onset and the time period of the oscillation. Moreover, we should like to point out that when the cavity was scanned slower, the oscillations endure much longer.

The instability described here is caused by two competing dynamic processes in the system, i.e., optical pumping from state $5S_{1/2}$ $F=2$ to state $5S_{1/2}$ $F=1$ by the controlling field and the nonlinear saturation effect between states $5S_{1/2}$ $F=1$ and $5P_{1/2}$ $F=2$ due to the interacting cavity field. This basic mechanism is similar to the one discussed in Ref. [3], but with a different experimental system. The oscillation time period is determined by the rates of these two dynamic processes, which are affected by the intensities and frequency detunings of the controlling and cavity fields. For example, as the controlling power increases, the optical pumping process starts to dominate, which reduces the rate of oscillation, as shown in Fig. 3. Likewise, as the intracavity power increases, the nonlinear saturation process dominates, giving rise to an increased oscillation rate, as shown in Fig. 4. The optical cavity plays an important role in the observed optical bistability and instability. It is the enhanced Kerr nonlinearity of the multilevel atomic medium together with the feedback mechanism through the optical ring cavity that produces such optical bistable behaviors. Furthermore, the index of refraction of the intracavity medium is altered by the optical pumping due to the controlling field (which increases the index of refraction) and by the saturation due to the intracavity field (which decreases the index of refraction). These changes of the index of refraction alter the effective cavity length (which is equivalent to scanning the cavity length back and forth) and, therefore, cause the cavity field to jump between two different steady states of the bistability, resulting in the observed self pulsing in our experiments. The relative strengths of the controlling and cavity fields and the rates of the two processes (optical pumping and saturation, which depend on the frequency detunings of the two fields) determine the oscillation time periods and amplitudes.

Although the Zeeman sublevels in the real atomic system used in the experiment are much more complicated than an ideal three-level Λ-type system, our previous experience with this atomic system indicates that an ideal three-level

Λ-type model is adequate to describe the basic physical behaviors of the real atomic system [6,7,12,13]. Moreover, the single-mode cavity field interacts with all atoms in the field mode collectively, so the spatial variation of the cavity field will not wipe out the oscillations that may have different time periods for different input cavity field intensities, as observed in Fig. 4. The key point here is that by controlling the experimental parameters (intensities and frequencies) of the controlling and cavity fields, we may control the transient population dynamics in this three-level atomic system. This kind of control was absent from the previous experimental system [3], where a single field causes the optical pumping and saturation of absorption. In our present experiment, we use two fields, a controlling field and a cavity field, to achieve greater control over bistability and instability. Four experimental parameters (the controlling power and its frequency detuning, and the cavity input power and its frequency detuning) may all be independently adjusted to explore the parameter space of the bistability and instability, which provides a good testing ground for many theoretical predictions of bistability and dynamic instability in multilevel atomic systems [14,15]. These observed oscillations could also relate to the photon blockade predicted in a four-level atomic system inside an optical cavity [16].

We have observed and studied bistability and instability in a three-level Λ-type atomic system inside an optical ring cavity. The bistability and instability may be independently controlled by adjusting the parameters (intensities and frequency detunings) of the controlling and cavity fields. Such control offers many advantages over the previous experimental system [3], where control is limited by the constraints of the experimental system. We explored the instability over large ranges of the parameter space and found the behaviors to be consistent with a simple theoretical model taking into account the transient behaviors of the atomic populations (optical pumping) as well as the transient behavior of the cavity field intensity in the optical ring cavity. Quantitative comparisons with complete theoretical calculations are needed to fully understand the observed dynamic behaviors of the system and are underway, which will help us to understand the dynamics of three-level atoms in an optical ring cavity under the influence of atomic coherence. Some interesting extensions of the current report include studying optical bistability at very low light levels, controlling optical bistability for an all-optical switch, and exploring chaotic behaviors of this system.

We acknowledge funding support from the National Science Foundation and the Office of Naval Research.

[1] L.A. Orozco, H.J. Kimble, A.T. Rosenberger, L.A. Lugiato, M.L. Asquini, M. Brambilla, and L.M. Narducci, Phys. Rev. A **39**, 1235 (1989).

[2] L.A. Orozco, A.T. Rosenberger, and H.J. Kimble, Phys. Rev. Lett. **53**, 2547 (1984).

[3] A. Lambrecht, E. Giacobino, and J.M. Courty, Opt. Commun. **115**, 199 (1995).

[4] S.E. Harris, Phys. Today **50**(7), 36 (1997); E. Arimondo, in *Progress in Optics XXXV*, edited by E. Wolf (Elsevier, Amsterdam, 1996), p. 257.

[5] K.J. Boller, A. Imamoglu, and S.E. Harris, Phys. Rev. Lett. **66**, 2593 (1991); J.E. Field, K.H. Hahn, and S.E. Harris, *ibid.* **67**, 3062 (1991).

[6] J. Gea-Banacloche, Y. Li, S. Jin, and M. Xiao, Phys. Rev. A **51**, 576 (1995); Y. Li and M. Xiao, *ibid.* **51**, R2703 (1995); M. Xiao, Y. Li, S. Jin, and J. Gea-Banacloche, Phys. Rev. Lett. **74**, 666 (1995).

[7] K. Hakuta, L. Marmet, and B.P. Stoicheff, Phys. Rev. Lett. **66**, 596 (1991).

[8] A.J. Merriam *et al.*, Phys. Rev. Lett. **84**, 5308 (2000); M. Jain, H. Xia, G.Y. Yin, A.J. Merriam, and S.E. Harris, *ibid.* **77**, 4326 (1996).

[9] P.R. Hemmer, D.P. Katz, J. Donoghue, M. Cronin-Golomb, M.S. Shahriar, and P. Kumar, Opt. Lett. **20**, 982 (1995).

[10] B. Lu, W.H. Burkett, and M. Xiao, Opt. Lett. **23**, 804 (1998); Y. Li and M. Xiao, *ibid.* **21**, 1064 (1996).

[11] M. Yan, E.G. Rickey, and Y. Zhu, Opt. Lett. **26**, 548 (2001).

[12] H. Wang, D.J. Goorskey, W.H. Burkett, and M. Xiao, Opt. Lett. **25**, 1732 (2000).

[13] H. Wang, D.J. Goorskey, and M. Xiao, Phys. Rev. Lett. **87**, 073601 (2001); H. Wang, D.J. Goorskey, and M. Xiao, J. Mod. Opt. (to be published).

[14] W. Harshawardhan and G.S. Agarwal, Phys. Rev. A **53**, 1812 (1996).

[15] L.M. Narducci, J.R. Tredicce, L.A. Lugiato, N.B. Abraham, and D.K. Bandy, Phys. Rev. A **33**, 1842 (1986).

[16] A. Imamoglu, H. Schmidt, G. Woods, and M. Deutsch, Phys. Rev. Lett. **79**, 1467 (1997).